INT. J. NUM. METH. HEAT FLUID FLOW, VOL. 2, 261–270 (1992)

FLOW OF A NEWTONIAN FLUID BETWEEN ECCENTRIC ROTATING CYLINDERS

ESTEBAN SAATDJIAN AND NOEL MIDOUX

Laboratoire des Sciences du Genie Chimique, ENSIC–LSGC, 1 Rue Grandville, BP 451, F-54001 Nancy Cédex, France

ABSTRACT

The flow between eccentric rotating cylinders when either the outer or inner cylinder is stationary is analysed both for the creeping flow approximation and for the case when inertial effects are not negligible. Numerical solutions are obtained using a finite difference ADI scheme and a fine orthogonal bipolar coordinate grid. When the centres of the two cylinders are far enough, a two-dimensional recirculation zone appears in the region where the gap spacing is greatest. On increasing the eccentricity, the recirculation zone becomes bigger and the separation and reattachment points move towards the region of narrowest gap. Further increase of the eccentricity results in the formation of a saddle point between the cylinders at the region of narrowest gap. As the Reynolds numbers increases, inertial effects modify slightly the recirculation region; the separation point moves upstream and the reattachment point moves downstream when either the inner or the outer cylinder rotate.

KEY WORDS Finite differences Bipolar coordinates Stokes flow Inertial flow

INTRODUCTION

The flow between eccentric rotating cylinders is one of the cases discussed by Taylor[14]. In lubrication theory, the clearance ratio (related to the radius difference between the inner and outer cylinders) is very small; since this parameter represents the characteristic length for this problem, the Reynolds number is usually much lower than 1 and inertial terms can be neglected safely. Early theoretical work on this problem was devoted to obtaining analytical solutions to the Stokes equations in a bipolar coordinate system. Wannier[1], Kamal[2] and others have obtained solutions to the biharmonic equations for the stream function.

For the case when the outer cylinder is stationary, Kamal[2] perturbed the Stokes flow solution to estimate inertial effects. In order to determine the criteria for the appearance of Taylor vortices in this geometry, he performed experiments and obtained visually that the transitional critical Taylor number is always above the one obtained for the concentric case and increases on increasing eccentricity. This latter result is in agreement with the later analysis of DiPrima and Stuart[3] but contradicts local stability theory. The first order inertial correction of Kamal gives results which completely modify the streamline pattern. Ritchie[4] obtained a critical Taylor number decrease for low eccentricities. Ballal and Rivlin[5] point out that Kamal's perturbation analysis is erroneous, they obtain a first order inertial correction to this flow. These authors find that the stream lines in the inertial case are just slightly different from the ones obtained from the Stokes solution.

More recently, San Andres and Szeri[6] solved the fourth order stream function equation numerically using a Galerkin method with B-splines. Although these authors mention that they could not obtain accurate results at high eccentricities, they show that the rotational sense of the separation and reattachment points given by Ballal and Rivlin[5] are erroneous in some cases.

0961–5539/92/030261–10$2.00

Received June 1991

One possible reason for this discrepancy is the fact that the inertial correction[5] does not satisfy the boundary conditions[6].

When the radius ratio is not small, inertial effects cannot be neglected. This flow is a test case in the study of mixing; Ottino[7] uses the available Stokes flow solutions to examine conditions which could lead to chaotic mixing of two viscous fluids, which is accomplished by time periodic movement of both cylinders. Today, this flow geometry is widely studied because of its applications both in lubrication and mixing phenomena.

Here, the flow between eccentric rotating cylinders is studied at both low (creeping flow) and high (inertial flow) Reynolds numbers. A finite difference numerical solution is obtained for both cases and compared with the available analytical and numerical work in the literature. At large clearance ratios the Stokes flow solutions vary, on increasing eccentricity, in a way that has yet to be discussed fully in the literature.

GOVERNING EQUATIONS

Consider the annular region between two eccentric cylinders; apart from the radii of both cylinders, the angular velocities of the rotating cylinders and the fluid properties, one further parameter is required to specify this flow problem: the distance between the centres of the cylinders. The difference between this problem and the axi-symmetric case first discussed by Taylor[8] can be resumed thus.

For the annular space between two eccentric cylinders, different orthogonal coordinate systems have been used. Ritchie[4], Ballal & Ritchie[5], and San Andres & Szeri[6] used the cylindrical bipolar coordinate system that is also used here. The transformation from Cartesian coordinates (x, y, z) to cylindrical bipolar coordinates (u, v, z) is effected by:

$$x = \frac{-a \sinh u}{\cosh u - \cos v} \qquad y = \frac{a \sin v}{\cosh u - \cos v} \qquad z = z$$

The Lamé coefficients are $(h, h, 1)$ where:

$$h = \frac{a}{\cosh u - \cos v}$$

For this coordinate system, if the inner and outer cylinders correspond to the $u = u_1$ and the $u = u_2$ curves, then the following relations can be derived:

$$R_1 = \frac{-a}{\sinh u_1} \qquad R_2 = \frac{-a}{\sinh u_2}$$

$$a = \frac{R_2 - R_1}{2\varepsilon}\left[\left(\frac{R_1 + R_2}{R_2 - R_1} - \varepsilon^2\right)^2 - \frac{4\varepsilon^2 R_1^2}{(R_2 - R_1)^2}\right]^{1/2}$$

$$\varepsilon = \frac{\sinh(u_1 - u_2)}{\sinh u_1 - \sinh u_2}$$

In the above equations, ε is the eccentricity ratio and represents the distance between the two cylinder centres divided by their radius difference.

The equations of motion lead, in dimensional form, to the following vorticity–stream function formulation:

$$\frac{\partial \omega}{\partial t} + \frac{U}{h}\frac{\partial \omega}{\partial u} + \frac{V}{h}\frac{\partial \omega}{\partial v} = \frac{\nu}{h^2}\left[\frac{\partial^2 \omega}{\partial u^2} + \frac{\partial^2 \omega}{\partial v^2}\right] -$$

$$h^2 \omega = \left[\frac{\partial^2 \psi}{\partial u^2} + \frac{\partial^2 \psi}{\partial v^2}\right]$$

where U and V are the velocity components in the u and v directions respectively and are

calculated from the stream function definition:

$$hU=\frac{\partial\psi}{\partial v} \qquad hV=-\frac{\partial\psi}{\partial u}$$

The following dimensionless variables are defined in order to normalize the governing equations:

$$u^*=\frac{u-u_1}{u_2-u_1} \qquad v^*=\frac{v}{2\pi} \qquad h^*=\frac{h}{a} \qquad \psi^*=\frac{\psi}{R_n^2\Omega_n}$$

$$U^*=\frac{2\pi aU}{R_n^2\Omega_n} \qquad V^*=\frac{a\Delta V}{R_n^2\Omega_n} \qquad \Delta=u_2-u_1 \qquad \omega^*=\frac{a^2\Delta^2\omega}{R_n^2\Omega_n}$$

where R_n is the radius of the rotating cylinder.

The dimensionless equations can then be written as:

$$\frac{\partial\omega^*}{\partial t^*}+\frac{U^*}{h^*}\frac{\partial\omega^*}{\partial u^*}+\frac{V^*}{h^*}\frac{\partial\omega^*}{\partial v^*}=\frac{1}{h^{*3}Re}\left[\left(\frac{2\pi}{\Delta}\right)\frac{\partial^2\omega^*}{\partial u^{*2}}+\left(\frac{\Delta}{2\pi}\right)\frac{\partial^2\omega^*}{\partial v^{*2}}\right]-$$

$$h^{*2}\omega^*=\left[\frac{\partial^2\psi^*}{\partial u^{*2}}+\frac{\partial^2\psi^*}{\partial v^{*2}}\right]$$

$$h^*U^*=\frac{\partial\psi^*}{\partial v^*} \qquad h^*V^*=-\frac{\partial\psi^*}{\partial u^*}$$

Apart from h^* and $\Delta/2\pi$ (which are related to the geometry), the only other dimensionless quantity appearing above is the Reynolds number defined by:

$$Re=\frac{R_n^2\Omega_n}{\nu}$$

The boundary conditions that are applied for the case when the outer cylinder is rotating at constant angular velocity are in dimensionless form:

$$U^*=V^*=0 \quad \text{for } u^*=0$$

$$U^*=0; \qquad V^*=\frac{a\Delta}{R_2} \quad \text{for } u^*=1$$

The boundary conditions for the case when the inner cylinder turns are easily deduced from the above. The symmetry condition leads to:

$$U^*=0 \quad \text{for } v^*=0 \quad \text{and } v^*=1$$

Before solving the above system of dimensionless equations numerically, a brief summary of the special case when the inertial terms can be neglected is given.

STOKES FLOW EQUATIONS

Analytical solution

When the Reynolds number is much less than 1, the creeping flow equations in bipolar coordinates are, in dimensional form:

$$\frac{\partial^2\omega}{\partial u^2}+\frac{\partial^2\omega}{\partial v^2}=0$$

$$-h^2\omega=\frac{\partial^2\psi}{\partial u^2}+\frac{\partial^2\psi}{\partial v^2}$$

In terms of the stream function, the two above equations can be combined leading to the biharmonic partial differential equation:

$$\nabla^4\psi=0$$

which is to be solved in bipolar coordinates. As mentioned before, analytical solutions have been reported in the literature, a brief outline of how they were obtained is given below. Applying separation of variables to the vorticity equation, one obtains that ω is of the form:

$$\omega=\sum_{n=0}^{\infty} p_n \sinh nu \cos nv+\sum_{n=0}^{\infty} q_n \cosh nu \cos nv$$

where p_n and q_n are unknown coefficients since boundary conditions at the walls for the vorticity are not known. Since this problem is symmetric, the v-direction conditions which were applied to obtain the above form were:

$$\frac{\partial\omega}{\partial v}=0 \quad \text{for } v=0 \quad \text{and } v=\pi$$

The stream function equation can be solved by first applying the transformation:

$$\psi=h\phi=h[F_0(u)+F_1(u)\cos v]$$

where ϕ is a function of both u and v and F_0 and F_1 are functions of u only. Inserting the above forms as well as the form obtained for the vorticity into the stream function equation one can show that:

$$F_0(u)=A_0\sinh u+B_0\cosh u+D_0 u\sinh u+E_0 u\cosh u$$

$$F_1(u)=A_1+B_1 u+D_1\sinh 2u+E_1\cosh 2u$$

where A_0, B_0, D_0, E_0, A_1, B_1, D_1, E_1 are constants determined from the boundary conditions. For the case when the inner cylinder is turning at a constant velocity V, the conditions are:

$$\psi=\psi_0; \qquad \left.\frac{\partial\psi}{\partial u}\right|_{u=u_1}=-hV \quad \text{for } u=u_1$$

$$\psi=\psi_1; \qquad \left.\frac{\partial\psi}{\partial u}\right|_{u=u_2}=0 \quad \text{for } u=u_2$$

where ψ_0 and ψ_1 are constants to be determined. The procedure used to determine them is to fix the value $\psi=0$ on the stationary cylinder and to require that the pressure be periodic in the v direction and single valued. An expression is then obtained for ψ on the moving cylinder.

The expressions for the above constants are too lengthy to be reproduced here; however, the reader can refer to Wannier[1], Kamal[2], or Ballal and Rivlin[5].

Numerical solution

The above dimensionless equations are solved numerically using finite differences. *Figure 1* shows a bipolar coordinate grid for $R_2/R_1=3$ and $\varepsilon=0.5$. The computer code written to solve both the inertial and the Stokes flow problems solves the equations in all the domain. For the creeping flow case, it could be possible to draw a horizontal symmetry line cutting both cylinders in half. The vorticity transport equation was solved by an ADI scheme with central, second order differences[12]. The stream function equation was also solved by an ADI scheme, the parameter sequence given by Wachpress[11] was employed. With this scheme, the user must be very careful in choosing the grid size. For a given radius ratio, the number of grid points in the u direction was chosen. As the eccentricity ratio is increased, the number of grid points in the v direction that will lead to convergence is seen to vary. Typical grid sizes employed are 21×201, 31×181 and 41×201 for $R_2/R_1=2$, 3, and 4 respectively. Only qualitative evidence can be put

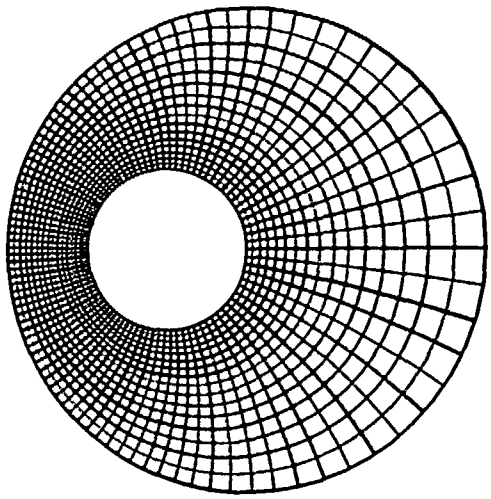

Figure 1 Bipolar coordinate grid for $R_2/R_1=3$ and $\varepsilon=0.5$

forward to show that the grid is fine enough. In a recent paper, Fant *et al.*[9] studied natural convection between horizontal concentric cylinders, the normalized gap width $((R_2-R_1)/R_1)$ varied from 0.1 to 1. Using a 31×101 grid for half the annular region they showed the appearance of multicellular flows at high Rayleigh numbers. Previous calculations with a coarser grid had been unable to show this result. Even though this problem is different from the one considered here, there is a mathematical analogy between them (see Drazin and Reid[10]). For example, linear stability theory leads to the same equations in Cartesian coordinates.

When the inertial flow equations are solved, a small Reynolds number ($Re=5$) is first solved. The obtained results are then used as starting point for the next value of Re; this procedure helps in reducing CPU time. The program stops when the two convergence tests have been successfully passed. The difference between calculated values of the stream function at all the grid points in both walls must not exceed 10^{-7} in relative value. Finally the vorticity everywhere must be constant from one step to the next, a 10^{-5}–10^{-7} relative error was tolerated depending on the Reynolds number. The numerical scheme was discussed in Saatdjian *et al.*[13]. All the boundary conditions are satisfied by this numerical scheme. It should be noted that a value of the stream function (for example $\psi=0$ was not chosen for the stationary cylinder because it does not automatically ensure that $V=0$ on that wall).

The accuracy of this numerical scheme does not depend on the system geometry, an advantage over the one used by San Andres and Szeri[6] who employed a B-spline Galerkin method. These authors state that for high eccentricity ratios the number of required terms in their series development was too big for their computer to handle. Here, only the total number of steps necessary for convergence increases when either the eccentricity ratio or the Reynolds number is increased.

RESULTS FOR STOKES FLOW

The Stokes flow solutions when either the inner or outer cylinder turns are first discussed. Although this may seem as a trivial matter due to the availability of analytical solutions, the author has not yet found a full discussion of the flow patterns in the literature. The reason may be that in lubrication, only small clearance ratios and eccentricities are of practical interest.

Consider the case when the outer cylinder turns at constant velocity, the radius ratio is equal

to 2. For low eccentricity ratio, the stream lines are almost circular and no recirculation zone exists; this is shown in *Figure 2a* for $\varepsilon=0.5$. above a certain value of ε (the value is a function of the clearance ratio), a recirculation zone appears in the flow. The streamline which separates the two-dimensional zone from the rest of the flow is the $\psi=0$ streamline. A typical case is shown in *Figure 2b* where $\varepsilon=0.7$. The two points where the $\psi=0$ streamline intersects the inner cylinder are called the separation and reattachment points. Further increase of ε leads to a radical change in the flow pattern. For $\varepsilon=0.75$ (*Figure 2c*) the two-dimensional zone becomes much bigger and both the separation and reattachment points move, symmetrically, towards the back of the inner cylinder.

If ε is increased even further, as shown in *Figure 2d* and *2e* where $\varepsilon=0.8$ and 0.9 respectively, a saddle point is obtained in the region where the gap is narrowest and only a very small layer of fluid turns in the same direction as the outer cylinder. Saddle points have been discussed by Ottimo[7] and Ballal and Rivlin[5] for this flow when both cylinders turn in opposite directions. The striking phenomenon at first occurring in these last two Figures is that although the outer cylinder is turning in one direction, the net flow is in the opposite direction. The above variation of the flow pattern on increasing ε has also been observed for $R_2/R_1=3$ although the transitions occur at different values of the eccentricity ratio.

When the inner cylinder turns, a two-dimensional recirculation zone appears on the outer cylinder at a lower value of ε. This is shown in *Figure 3a* for the same radius ratio ($R_2/R_1=2$) as before and for $\varepsilon=0.5$. Again, the $\psi=0$ streamline separates the two flow regions. As ε is increased, the separation and reattachment points move towards the region of narrowest gap and the recirculation zone becomes bigger. This is shown in *Figure 3b* and *3c* where $\varepsilon=0.7$ and 0.75 respectively. Further increase of ε leads to a saddle point in the region of minimum clearance as shown in *Figure 3d* and *3e* where $\varepsilon=0.8$ and 0.9 respectively. As in the case when the outer cylinder rotates discussed above, the net flow in *Figure 2d* and *2e* is in a direction opposite to the one of the cylinder rotation. Again, a similar behaviour is observed for other radius ratios.

The above Stokes flow results differ from those obtained by Ballal and Rivlin[5] in some cases but not all. For example, for the case of rotating inner cylinder, the streamline pattern for $\varepsilon=0.5$ is identical in both cases. However, at lower or higher values of ε the results do not match. When the inner cylinder rotates, the value of ε for which a two-dimensional zone appears at

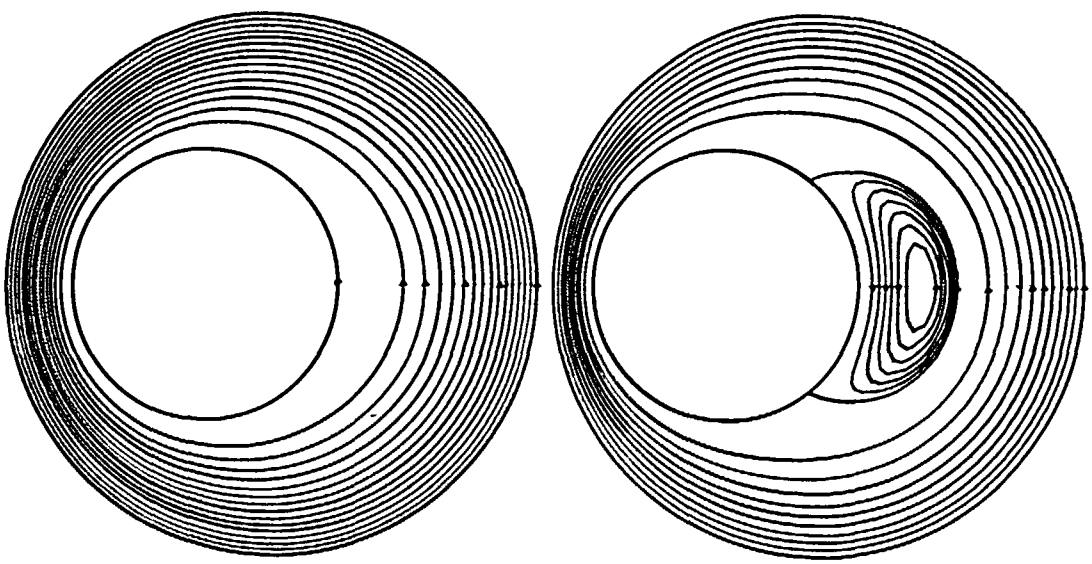

Figure 2 Streamlines for Stokes flow when the outer cylinder rotates, $R_2/R_1=2$. (a) $\varepsilon=0.5$, (b) $\varepsilon=0.7$, (c) $\varepsilon=0.75$, (d) $\varepsilon=0.8$, (e) $\varepsilon=0.9$

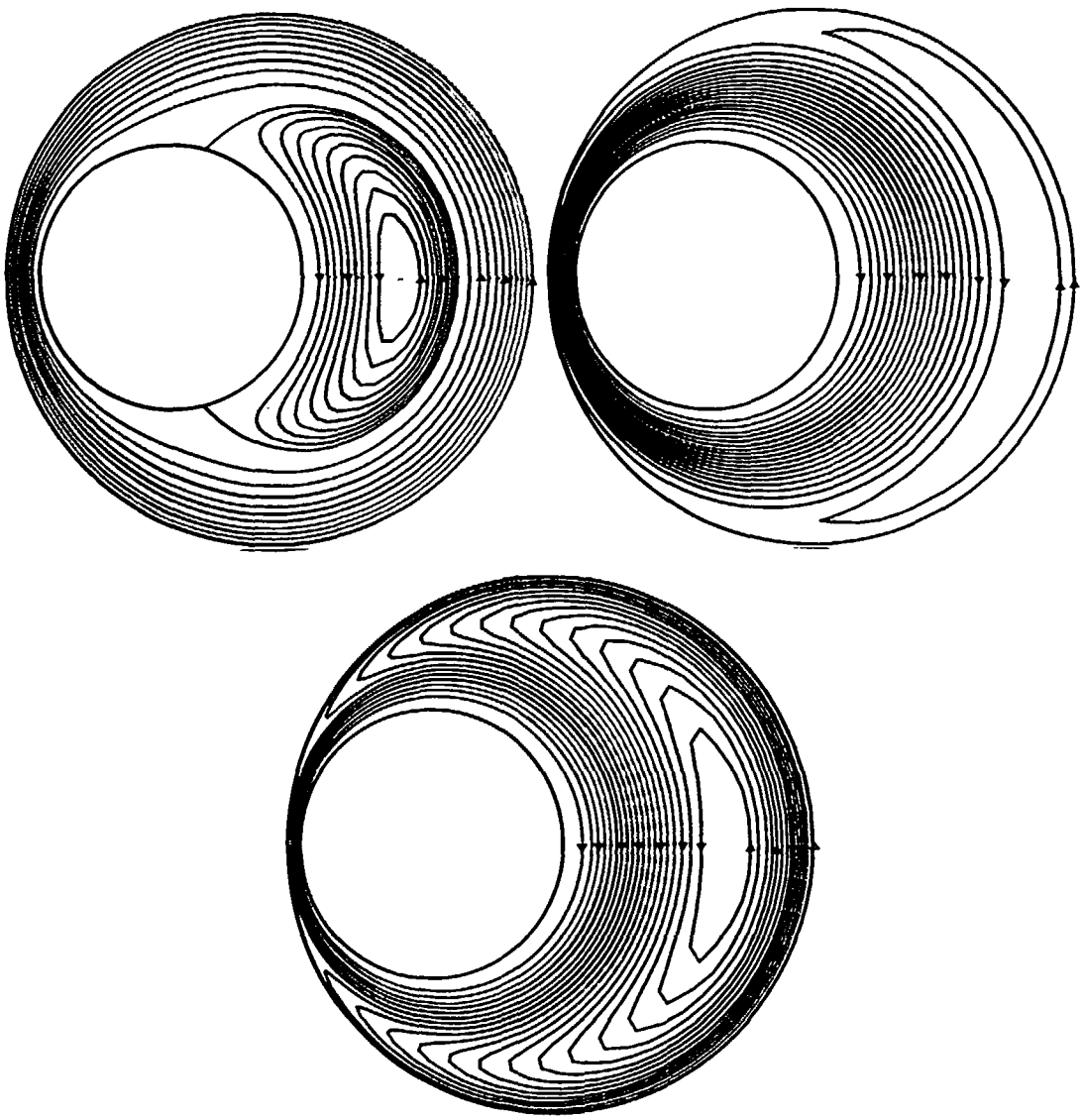

Figure 2 (continued)

$R_2/R_1 = 2$ is slightly less than 0.2. This result is in agreement with the numerical calculations of San Andres and Szeri[6] but is lower than the value obtained using the analytical solution[5]. This discrepancy could be due to the analytical calculation of the value of ψ at the moving wall.

The above comments apply also to the case when the outer cylinder rotates. The value of ε obtained here, for a vortex zone to appear is 0.53 instead of 0.27. Again the value given by Reference 5 could be questioned because it is lower than that for the case when the inner cylinder rotates. In the concentric case, it is well known that a rotating inner cylinder is less stable than a rotating outer cylinder; Taylor vortices appear at a lower value of the Reynolds number.

In all the above numerical calculations, a 10^7 relative error on both the stream function and the vorticity was obtained. The calculations required approximately 1500 time steps and about 15 min CPU time on a RISC 6000 workstation.

INERTIAL EFFECTS

The influence of inertia on this flow is analysed by solving the full Navier–Stokes equations given above. The CPU time necessary to obtain results for given geometry and Reynolds number increases drastically; a typical run, for the same convergence criteria as before requires about 5 hours on the same computer. The grid sizes used are the same as before and depend on the considered radius and eccentricity ratios. The Reynolds numbers considered below are below the critical value leading to a three dimensional flow similar to the toroidal vortices observed by Taylor[8].

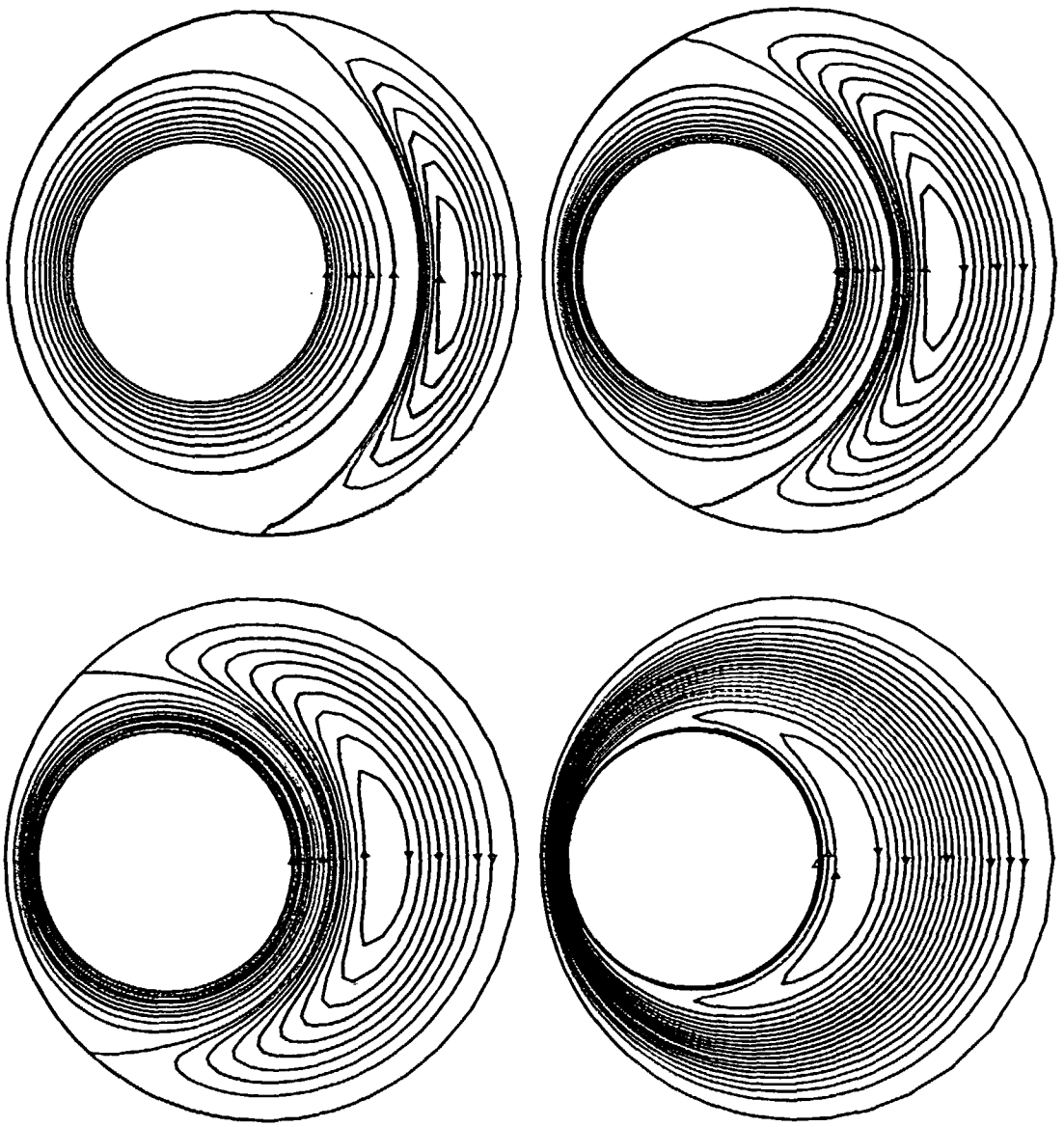

Figure 3 Streamlines for Stokes flow when the inner cylinder rotates, $R_2/R_1=2$. (a) $\varepsilon=0.5$, (b) $\varepsilon=0.7$, (c) $\varepsilon=0.75$, (d) $\varepsilon=0.8$, (e) $\varepsilon=0.9$

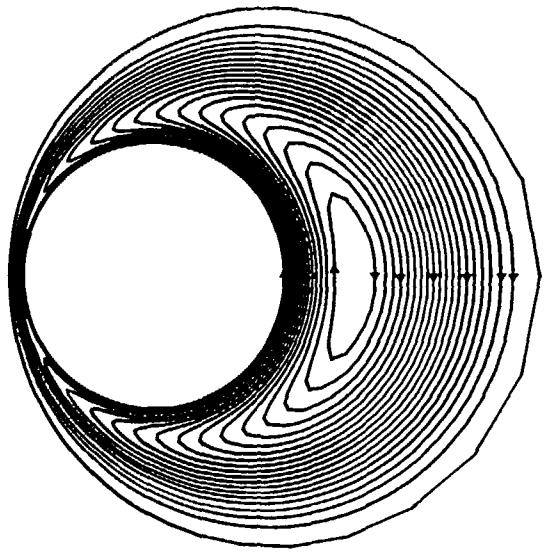

Figure 3 (*continued*)

When inertial effects are taken into account, the flow pattern is no longer symmetrical and the centre of the two-dimensional zone moves in the direction of the cylinder displacement. This is shown in *Figure 4* where streamlines for both Stokes and inertial flow ($Re=20$) are shown. The geometrical parameters are $R_2/R_1=3$ and $\varepsilon=0.7$, and the outer cylinder is turning at constant velocity. The separation point moves upstream and the reattachment point moves downstream, as shown in *Figure 4*. This result is in contradiction with both the inertial correction of Ballal and Rivlin[5] and with the numerical calculations of San Andres and Szeri[6]. San Andres and Szeri[6] state that the inertial correction[5] does not satisfy the correct boundary conditions. San Andres and Szeri also state in their paper that their numerical code breaks down at high eccentricity although they do not give an exact value of ε.

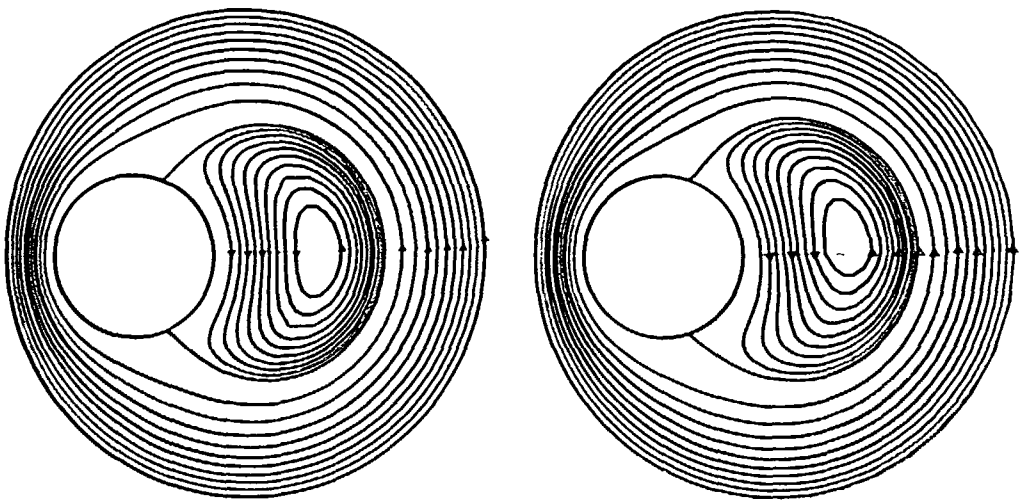

Figure 4 Streamlines for inertial flow when the outer cylinder rotates, $R_2/R_1=3$, $\varepsilon=0.7$. (a) Stokes flow, (b) $Re=20$

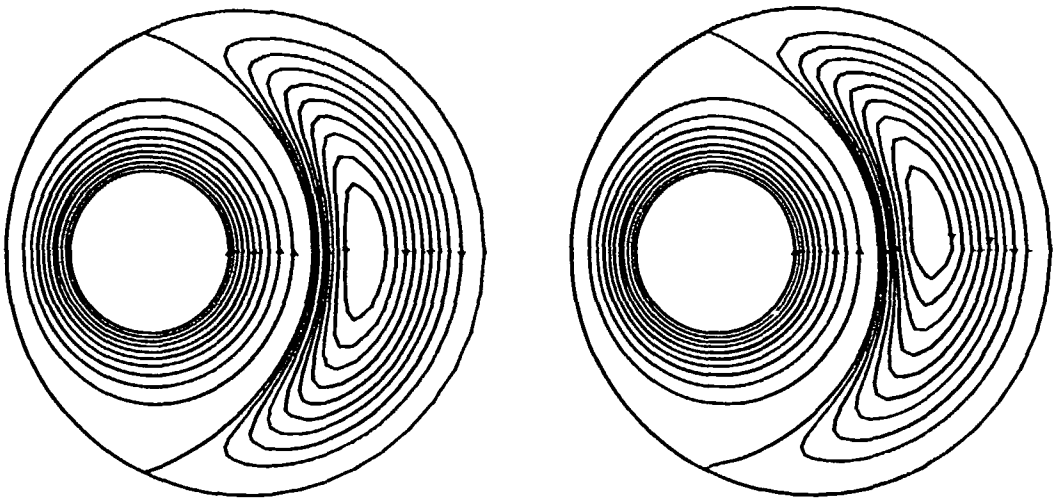

Figure 5 Streamlines for inertial flow when the inner cylinder rotates, $R_2/R_1=3$, $\varepsilon=0.6$. (a) Stokes flow, (b) $Re=20$

Figure 5 shows a similar comparison for $R_2/R_1=3$, $\varepsilon=0.6$ and the inner cylinder turning. The solution for $Re=20$ shows that inertial effects tend to stretch the size of the two-dimensional vortex zone.

CONCLUSIONS

The flow between eccentric rotating cylinders has been solved numerically both for low and high Reynolds numbers. The finite difference scheme used on grids containing approximately 5000 points has been tested against an available analytical solution for the creeping flow case. The finite difference code developed allows the user to treat all geometries; this is particularly important in mixing where high clearance and eccentricity ratios are common. The flow regime is seen to change dramatically on increasing the eccentricity ratio and saddle points can be present when only one cylinder turns. For a given geometry, an increase of the turning cylinder velocity is seen to lead to a stretching of the two-dimensional region.

REFERENCES

1 Wannier, G. A contribution to the hydrodynamics of lubrication, *Q. Appl. Math.*, **8**, 1–32 (1950)
2 Kamal, M. Separation in the flow between eccentric rotating cylinders, *J. Basic Eng.*, **88**, 717–724 (1966)
3 Di Prima, R. C. and Stuart, J. T. The non-linear calculation of Taylor-vortex flow between eccentric rotating cylinders, *J. Fluid Mech.*, **54**, 393–415 (1975)
4 Ritchie, G. S. On the stability of viscous flow between eccentric rotating cylinders, *J. Fluid Mech.*, **32**, 131–144 (1968)
5 Ballal, B. and Rivlin, R. S. Flow of a Newtonian fluid between eccentric rotating cylinders, *Arch. Rational Mech. Anal.*, **62**, 237–294 (1977)
6 San Andres, A. and Szeri, A. Flow between eccentric rotating cylinders, *J. Appl. Mech.*, **51**, 869–878 (1984)
7 Ottino, J. M. *The Kinematics of Mixing: Stretching, Chaos and Transport*, Cambridge Univ. Press, Cambridge (1989)
8 Taylor, G. I. Stability of viscous liquid contained between two rotating cylinders, *Proc. R. Soc.*, **A223**, 289–343 (1923)
9 Fant, D. B. *et al.* Natural convective flow instability between horizontal concentric cylinders, *Numerical Methods in Laminar and Turbulent Flow*, Vol. 6, Part 2, pp. 1947–1965, Pineridge Press, Swansea (1989)
10 Drazin, P. G. and Reid, W. H. *Hydrodynamic Stability*, Cambridge Univ. Press, Cambridge (1981)
11 Wachpress, E. *Iterative Solution of Elliptic Systems*, Prentice-Hall, New York (1966)
12 Roache, P. J. *Computational Fluid Dynamics*, Hermosa, Albuquerque, NM (1982)
13 Saatdjian, E. *et al.* Numerical simulation of flow between eccentric rotating cylinders, *Numerical Methods in Laminar and Turbulent Flow*, Vol. 7, Part 1, pp. 433–442, Pineridge Press, Swansea (1991)
14 Taylor, G. I. *Low Reynolds Numbers Flows*, National Committee for Fluid Mechanics Films, Cambridge University (1966)